Desalination and Water Treatment
www.deswater.com

doi:10.5004/dwt.2019.23308

139 (2019) 288–296
January

Facile preparation of mercapto modified magnetic iron oxide nanoparticles for removal of mercury(II) from aqueous solutions

Yuehong Pang, Qin Wang, Yun Ma, Qi Yue, Xiaofang Shen*

State Key Laboratory of Food Science and Technology, School of Food Science and Technology, Jiangnan University, Wuxi, 214122, China, Tel. +86-510- 85916906, Fax +86-510-85329081, email: yhpang@jiangnan.edu.cn (Y. Pang), 279243242@qq.com (Q. Wang), 871901448@qq.com (Y. Ma), 476419547@qq.com (Q. Yue), xfshen@jiangnan.edu.cn (X. Shen)

Received 13 May 2018; Accepted 18 October 2018

ABSTRACT

A simple ultrasound-assisted co-precipitation method was developed to prepare lipophilic thiol-functionalized Fe_3O_4 magnetic nanoparticles (EDT-Fe_3O_4 MNPs) with sodium dodecyl sulfonate (SDS) as dispersant and 1,2-ethanedithiol (EDT) as functionalization reagent. The property of EDT-Fe_3O_4 MNPs was characterized by Fourier transform infrared spectroscopy (FTIR), energy dispersive spectroscopy (EDS), X-ray powder diffraction (XRD), transmission electron microscope (TEM), vibrating sample magnetometer (VSM) and thermogravimetric analysis (TGA). It was found that EDT-Fe_3O_4 MNPs dispersed well in the system of ethanol/water (1:1) and had an average diameter of 15 nm. The hysteresis loop of EDT-Fe_3O_4 MNPs demonstrated that these MNPs expressed high magnetic responsiveness. The EDT-Fe_3O_4 MNPs were further used as an adsorbent for removal of Hg^{2+}. The effects of the dosage of adsorbent, initial pH of the solution and contact time were investigated. The adsorption equilibrium and kinetics data could be well fitted with the Freundlich isotherm and the pseudo-first-order kinetic model respectively. Furthermore, the adsorbent could be effectively separated using an external magnetic field and regenerated.

Keywords: Mercury(II) removal; Mercapto modified; Fe_3O_4 nanoparticles; Magnetic separation

1. Introduction

Heavy metals, though essential for industry, have been recognized as major pollutants to plants, animals and human beings for their highly toxic, non-biocompatible traits [1]. Mercury is a typical hypertoxic heavy metal and hazardous substance to cause accidental pollution events, such as Minamata disease in Japan and it has been regarded as one of "the priority hazardous substances" by the Agency for Toxic Substances and Disease Registry [2,3]. Mercury poisoning is a serious threat to human health, and global mercury emissions continue to rise at an alarming pace [4]. Solid waste incineration and the combustion of fossil fuels are significant sources of mercury emissions [5]. It is worth to note that once mercury has been introduced into the aquatic ecosystem,some aquatic bacteria in the water sediments could convert the mercury ion to the very toxic compound methyl mercury which could readily accumulate in human body [6]. As a consequence, a series of damages and subsequent diseases will be caused, such as neurological and renal dysfunctions, serious cognitive and motion disorders, hepatic injury, hydrargyriasis disease, Amyotrophic lateral sclerosis and Alzheimer's diseases [3,7–9]. Therefore, in the field of environmental engineering and health control, removal of Hg^{2+} is undoubtedly of great importance.

To date, adsorption, ion exchange, amalgamation, and chemical precipitation are a few of the available techniques for the removal of mercury and other heavy metal ions from contaminated water [10–13]. Relatively, adsorption is considered to bean effective and economical method for removal mercury ions. Different types of absorbents have been proposed including active carbon [14], noble nanoparticles [15,16] mesoporous materials [17,18], polymer [19,20] and biosorbents [21,22]. Recently, organically functionalised

*Corresponding author.

magnetic nanoadsorbents have been receiving a great deal of attention in this field.

Adsorbents based on strong Hg-S bonding, such as 2-aminothiazole, dimethyl sulfoxide, dithizone, 2-mercaptobenzimidazole, 6-mercaptopurine, and thiosemicarbazide are commonly used for removing mercury ions from natural water [23–25]. Most of these mercapto functionalized matierals was used in solid phase extraction (SPE). However, tedious and complicated processes are required to prepare these adsorbents, and thus, they are typically costly.

A distinct advantage of magnetic separation is that magnetic nanoparticales can be efficiently isolated from sample solutions by the application of an external magnetic field. Generally, most of the dissolved environmental contaminants are nonmagnetic, and thus do not respond to a magnetic field. Furthermore, magnetic nanoparticles possess large surface areas and have unique magnetic properties. High efficient removal of Hg^{2+} from complex environmental matrices can be obtained when functional mercapto ligands are bounded onto these magnetic nanoparticles. The primary aim of this work is to demonstrate a simple strategy for removal of Hg^{2+} from water based on our magnetic Fe_3O_4 nanoparticles (Fig. 1). Our facile approach takes advantage of the strong affinity with Hg^{2+} and mercapto modified Fe_3O_4 nanoparticles.

2. Experimental

2.1. Materials

$FeSO_4{\cdot}7H_2O$, $FeCl_3{\cdot}6H_2O$, $NH_3{\cdot}H_2O$, ethanol, 1,2-ethanedithiol (EDT), sodium dodecyl sulfonate (SDS) obtained from Aladdin reagent (Shanghai, China) were of analytical reagent grade or better quality and used as received without further purification. Ultrapure water was used throughout the experiment. The aqueous solution of Hg^{2+} (1 mg/mL) was prepared daily by using $HgCl_2$ (Merck, Darmstadt, Germany). More diluted mercury solutions were prepared with step-by-step dilution of concentrated mercury solutions.

2.2. Synthesis procedure of the mercapto modified Fe_3O_4 nanoparticles

The preparation of the aqueous magnetic Fe_3O_4 nanoparticles was based on co-precipitation of Fe^{2+} and Fe^{3+} salts in alkali aqueous medium (NH_4OH) under ultrasound irradiation. Since the as-synthesized nanoparticles show a strong tendency to agglomerate, they have to be dispersed prior to their coating with EDT. A stable aqueous suspension of super paramagnetic Fe_3O_4 nanoparticles was prepared using SDS as the surfactant through a procedure described [26]. In a typical synthesis, known molar ratios of Fe^{2+} salt, Fe^{3+} salt and SDS served as feed solutions. The reactor was filled with dry N_2 and the temperature of the whole reactor was maintained at 50°C. Continuous and homogeneous ultrasonic irradiation all over the solutions were provided by an ultrasonic reactor. The pH value in the solution is an imperative factor for controlling the chemical species and size distribution of the synthesized Fe_3O_4 particles. In this paper, the pH value in the reaction system was adjusted to 9 by pumping in $NH_3{\cdot}H_2O$ solution with a flow rate of 2 mL/min. Obtained Fe_3O_4 precipitate was aged at 80°C for 30 min in an ultrasonic water bath. To purify prepared Fe_3O_4 particles, the samples were washed repeatedly with ultrapure water and ethanol until pH level of 7 was reached.

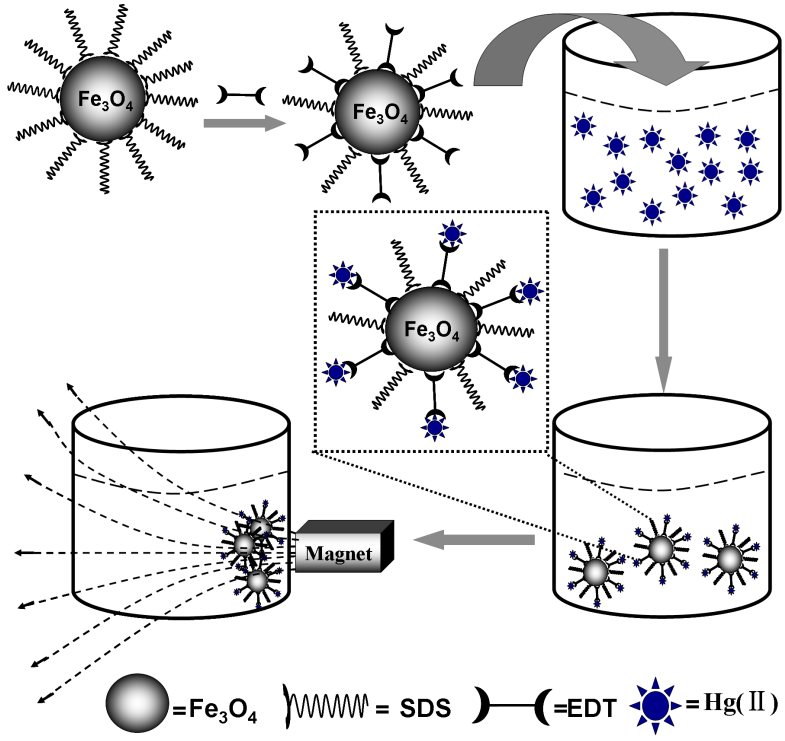

Fig. 1. The synthetic route of EDT-Fe_3O_4 MNPs and its magnetic separation of Hg^{2+}.

To obtain mercapto modified magnetic nanoparticles, ligand exchange reaction by EDT and SDS capped Fe_3O_4 nanoparticles was performed. The as-synthesized Fe_3O_4 nanoparticles were washed three times and dispersed in 40 mL ethanol. 580 µL EDT solution was added dropwise under ultrasound irradiation. After reaction for 20–30 min, the nanoparticles were collected by a magnetic field and washed three times with ethanol. The precipitant was then dried in vacuum for characterization.

2.3. Characterization

Transmission electron microscopy (TEM) was carried out using a field emission TEM (G2 F20 S-Twin, Tecnai,America) at 200 kV to measure the particle size and shape. Magnetic behavior was tested by a vibrating sample magnetometer (VSM) (7407, Lake Shore,America). The infrared spectrum was obtained using a Fourier Transform-Infrared Spectrometer (FT-IR, 470 spectrometer, Nicolet Nexus,America) to identify the functional groups and chemical bonding of the coated nanoparticles. X-ray diffraction measurements (D8 ADVANCE, Bruker, Germany) were conducted to investigate the crystal structure of the nanoparticles. The zeta potential and the hydrodynamic diameter of the nanoparticles was measured by dynamic lights scattering (ZetaSizer nanoZS, Malvern, England). Organic components of Fe_3O_4 nanoparticles were studied by thermal analysis-thermogravimetry (TGA/SDTA851e, Mettler-Toledo, Switzerland). The synthesis was under the ultrasonic irradiation (JYD-650L,Zhi Sun instrument, China). EDT solution was added with a Syringe Pump (LSP02-1B, Longer, China). The concentrations of Hg^{2+} solutions were measured on a dual beam UV-Vis Spectrophotometer (U-1900 Purkinje General, China).

2.4. Adsorption experiments

All adsorption experiments were performed at 25°C and repeated at least twice to ensure accuracy of the obtained data. The adsorption of Hg^{2+} ions by EDT-Fe_3O_4MNPs are as follows (the process is shown in Scheme 1): 2 µmol/L of EDT-Fe_3O_4 MNPs were added to a 4 mL mercury-containing solution adjusted to pH 6 and mixed for several minutes at a 500 rpm agitation speed.0.1 mol/L HCl and 0.1 mol/L NaOH solutions were used for pH adjustment. Then the magnetic adsorbent was removed magnetically from the solution with a permanent magnet. The adsorption time, solution pH, and adsorbent dose was changed to reveal their impacts on Hg^{2+} adsorption. The concentration of Hg^{2+} ions in the aqueous solution after adsorption was quantified by the colorimetric method of National Standard of China (GB/T 5750.6-2006) [27], at a wavelength of 485 nm, after a minor modification.

For the calculation of the mercury adsorption rate (R) by EDT-Fe_3O_4 MNPs, the following expression was used:

$$R(\%) = \frac{C_0 - C_t}{C_0} \times 100 \quad (1)$$

where C_0 denotes the initial concentration of Hg^{2+} and C_t is the concentration of Hg^{2+} at the time t [28].

3. Results and discussion

3.1. Preparation and characterization of EDT-Fe_3O_4 MNPs

The magnetically assisted chemical separation (MACS) process, in which researchers utilized magnetic nanoparticles coated with a selective functional groups for the efficient recovery of hazard materials, provides a useful method of decorporation based on magnetic nanoparticles [29]. Fig. 1 shows the synthetic route of mercapto conjugated Fe_3O_4 nanoparticles and magnetic separation of Hg^{2+}.

TEM was used to observe the morphology of the adsorbent. As shown in Fig. 2a, the as-prepared EDT-Fe_3O_4 MNPs are found to be quasi-spherical in shape, and have nearly uniform distribution of particle size. The average diameter of EDT-Fe_3O_4 MNPs was 15 nm. Elemental mapping analysis of the EDT-Fe_3O_4 MNPs was studied by EDS (Fig. 2b). Characteristic peaks are assigned to iron, sulphur, carbon and oxygen elements, which unanimously interprets that EDT anchors to the surface of Fe_3O_4 MNPs.

It has been reported that Fe_3O_4 particles with diameters smaller than 20 nm are likely to exhibit a superparamagnetic property [30,31]. Magnetic property of EDT-Fe_3O_4 MNPs was performed at room temperature using a vibrating sample magnetometer (VSM) in an external magnetic field, as shown in Fig. 3a. The saturation magnetization of EDT-Fe_3O_4 MNPs obtained from the hysteresis loop was 25 emu/g and the EDT-Fe_3O_4 MNPs exhibited negligible coercivities and remanence, which clearly indicates their superparamagnetic behavior [32]. The results reveal that-EDT-Fe_3O_4 MNPs can be separated rapidly from aqueous

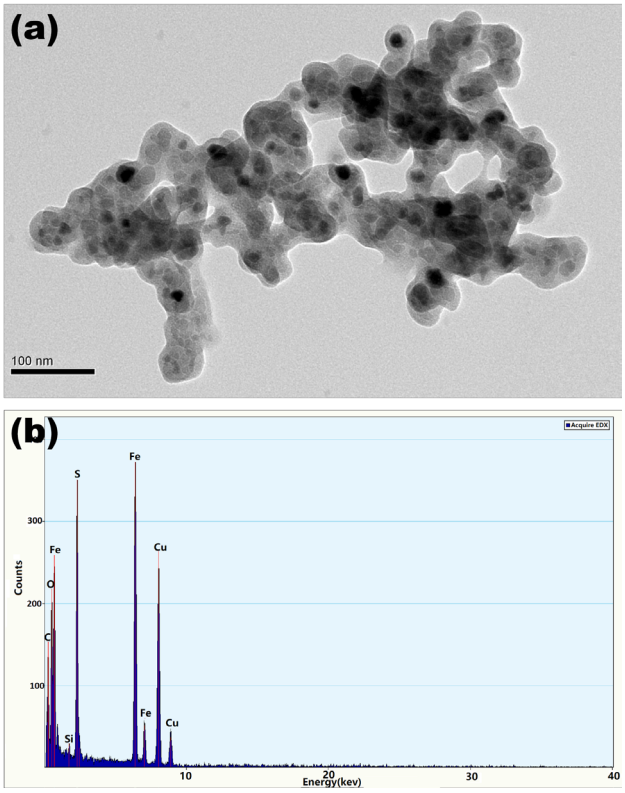

Fig. 2. (a) TEM and (b) EDS of EDT-Fe_3O_4 MNPs.

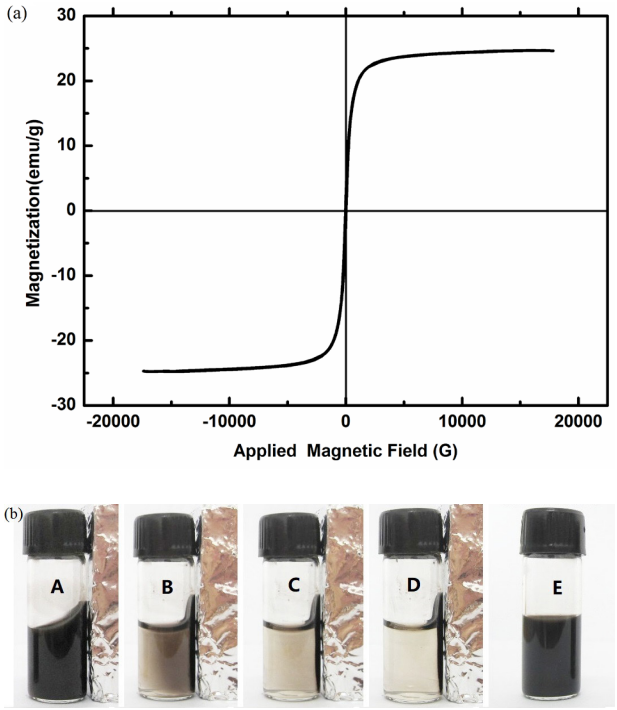

Fig. 3. (a) Magnetic hysteresis loop, and (b) Photographs of the separation (A to D) and redispersion (E) process of EDT-Fe_3O_4 MNPs.

solution because saturation magnetization of 16.3 emu/g is sufficient for magnetic separation with a conventional permanent magnet [33].

A significant advantage of MNPs with the superparamagnetic property for magnetic separation is that after aggregation by a magnetic field, the aggregated MNPs can be easily redispersed in solution upon removal of the magnetic field [32]. As shown in Fig. 3b, after dispersing the as-synthesized EDT-Fe_3O_4 MNPs, a magnet was used for separation. Upon removal of the magnetic field, the EDT-Fe_3O_4 MNPs were easily redispersed in water with slight shaking, suggesting their potential application of magnetic adsorbent.

The crystal structure of as-synthesized MNPs is presented in Fig. 4. Six characteristic peaks at 2θ = 30.2°, 35.4°, 43.2°, 53.8°, 57.1° and 62.8° are observed, which are ascribed to the (220), (311), (400), (422), (511) and (440) planes of Fe_3O_4, respectively [34]. The reflection peak positions and relative intensities of MNPs are well in agreement with the database of JCPDS 75-1609, confirming the resultant nanoparticles are pure $Fe_3O_4$with a spinel structure and the ligand exchanging process have no effect on the phase change. The XRD results also demonstrate high crystallinity of prepared Fe_3O_4 nanoparticles.

FTIR spectroscopy, a sensitive technique to detect the molecular vibrations, can be used to study the surface structures of the as-synthesized EDT-Fe_3O_4 MNPs. Fig. 5 shows the FTIR spectra of SDS-Fe_3O_4 MNPs (a) and EDT-Fe_3O_4 MNPs (b). The broad peaks centered at 3400 cm^{-1} and 613 cm^{-1} are attributed to the stretching vibrations of O-H bond from residual water in the samples and Fe-O bond. This peak for Fe-O was shifted to a higher wave-

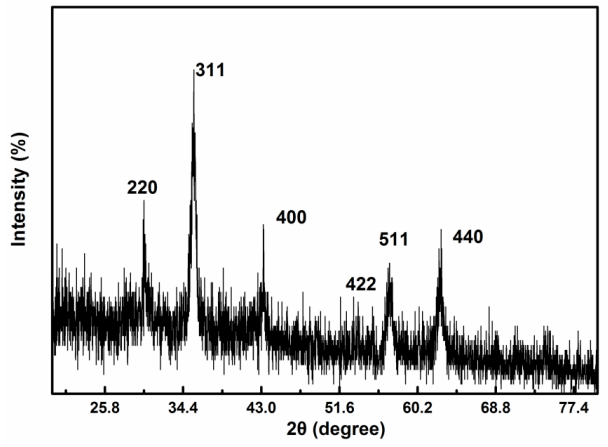

Fig. 4. XRD pattern of the EDT-Fe_3O_4 MNPs.

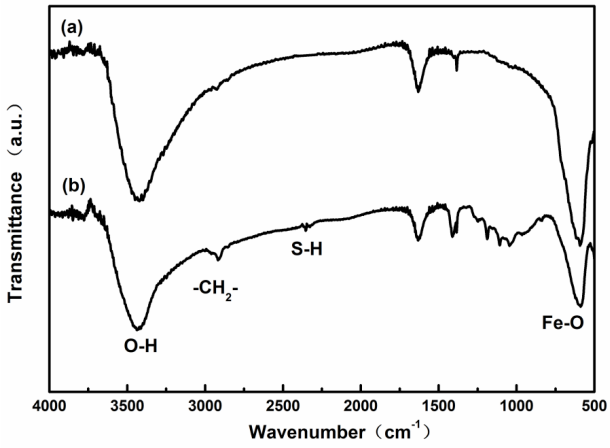

Fig. 5. FTIR spectra of (a) SDS-Fe_3O_4 MNPs, and (b) EDT-Fe_3O_4 MNPs.

number compared to the peak of bulk Fe_3O_4 MNPs, due to the modifying of SDS and EDT on the surface of Fe_3O_4 MNPs [35]. In the case of SDS-Fe_3O_4 MNPs (Fig. 5a), the absorption bands at 1643 cm^{-1} and 1386 cm^{-1} are related to the stretching vibrations of C-C and C-H, respectively. While in Fig. 5b, a new peak was appeared at 2370 cm^{-1} that indicated the S-H stretching of EDT moiety, revealing that the EDT has been successfully grafted onto the surface of Fe_3O_4 MNPs [36]. The peak observed at 2937 cm^{-1} correspond to the C-H stretching vibrations of the CH_2 group.

The thermal behavior of the SDS-Fe_3O_4 MNPs and-EDT-Fe_3O_4 MNPs were also monitored (Fig. 6). As shown in Fig. 6a, the weight loss for SDS-Fe_3O_4 MNPs over the temperature ranging from 100°C to 800°C is only about 3%, which can be ascribed to the loss of SDS on the surface of Fe_3O_4 MNPs. While the TGA curve for EDT-Fe_3O_4 MNPs (Fig. 6b) shows two weight change steps. Below 200°C, the weight loss is quite small due to the evaporation of physically adsorbed water in the sample. After that, there is an obvious weight loss of 13% from 200°C to 350°C, which may result from the decomposition of SDS and EDT on the surface of material. Taking this into

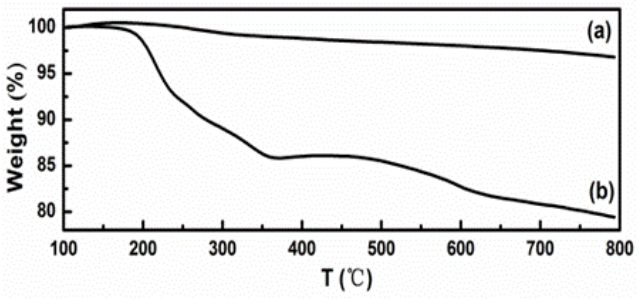

Fig. 6. TGA analysis of (a) SDS-Fe_3O_4 MNPs and (b) EDT-Fe_3O_4 MNPs.

account, we speculate that the EDT ligand has been successfully capped onto the surface of Fe_3O_4 MNPs, also supporting the FTIR analysis. Besides, the differences in total weight loss for both samples give evidence for calculating the percentage of EDT molecules attached to surface of nanoparticles. Thus it is implicit that about 10% of the EDT was adsorbed onto the surface of the nanoparticles. While the weight gain, beginning at around 400°C and completing by 500°C, could be attributed to the transformation from Fe_3O_4 toFe_2O_3. When the temperature is higher than 700°C, the weight remains basically unchanged suggesting that only iron oxide is present in this temperature range.

3.2. Adsorption properties

3.2.1. Effect of pH

The solution pH is one of the most important factors for the adsorption of heavy metal ions, since pH values determine not only the activity of adsorption sites on the adsorbent, but also the existing forms of heavy metal ions in solution. Therefore, it is highly significant to investigate the influences of solution pH on heavy metal ions adsorption. The effect of pH on Hg^{2+} removal using EDT-Fe_3O_4 MNPs was assessed at pH values ranging from 2 to 10. As is illustrated in Fig. 7, the removal efficiency decreased slightly with increasing solution pH. Mainly because, with the increase of solution pH, more and more Hg^{2+} get out of the solution to form insoluble colloidal metal hydroxide of $Hg(OH)_2$, thus inhibit the adsorption process and decreased the adsorption efficiency. Therefore, we used sample solutions at the optimal pH of 6.0 for further adsorption experiments.

3.2.2. Effect of contact time

The importance of contact time comes from the need for identifying the possible rapidness of binding and removal processes of the tested metal ions by the adsorbents and obtaining the optimum time for removal of the target metal ions. The effect of contact time on adsorption of Hg^{2+} onto EDT-Fe_3O_4 MNPs was carried out at 5–50 min as shown in Fig. 8. There were almost no significant changes in the adsorption efficiency from 5–50 min. This can be explained by the reduced availability of Hg^{2+} to active sites on the EDT-Fe_3O_4 MNPs surface.

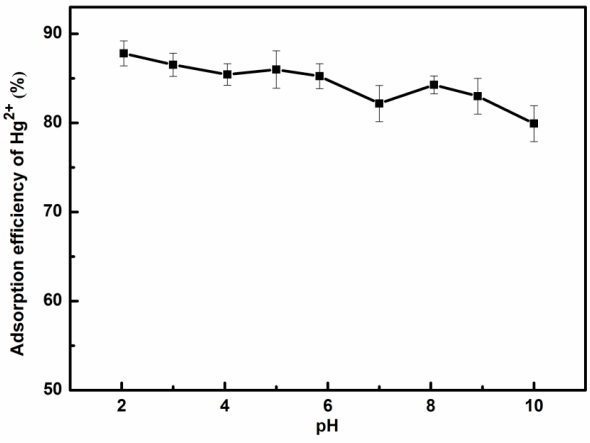

Fig. 7. Effect of pH on Hg^{2+} adsorption efficiency. Experiment conditions: 2 µmol adsorbents, 1.0 mg/L Hg^{2+} solution, 10 min contact time, 500 rpm agitation speed, room temperature.

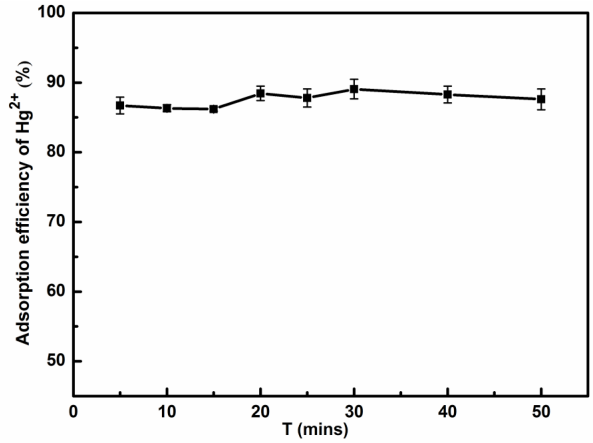

Fig. 8. Effect of adsorption time on Hg^{2+} adsorption efficiency. Experiment conditions: 2 µmol adsorbents, 1.0 mg/L Hg^{2+} solution, 500 rpm agitation speed, pH = 6.0, room temperature.

However, over 86.3% of Hg^{2+} could be removed within 10 min, indicating that the adsorption equilibriums were achieved quickly. Such a rapid adsorption rate could be attributed to the absence of internal diffusion resistance and this property is attractive for practical application. Therefore,optimum contact time for adsorption of Hg^{2+} was considered to be 10 min.

3.2.3. Effect of the adsorbent dosage

Due to their significantly high surface area and short diffusion route compared with other sorbents, nanoparticles can have high adsorption efficiency and fast adsorption dynamics. Thus satisfactory results with less adsorbent can be achieved with these sorbents. To investigate the effect of EDT-Fe_3O_4 MNPs amount, various concentrations of EDT-Fe_3O_4 MNPs in the range of 2–26 µmol at a fixed initial Hg^{2+} concentration of 1.0 mg/L were used to adsorb Hg^{2+} under the optimum condition (pH =

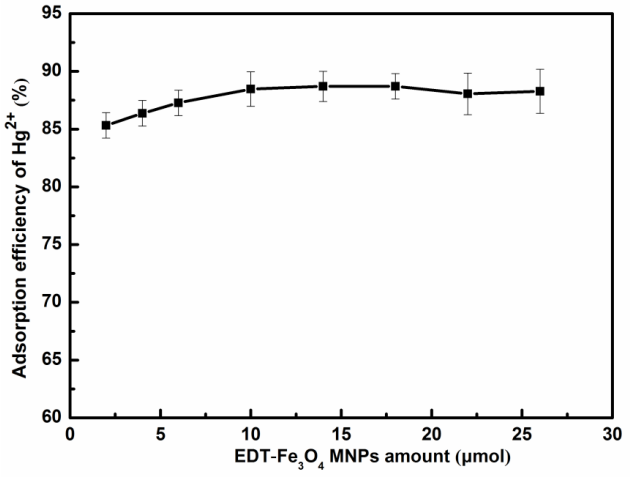

Fig. 9. Effect of adsorbent dosage on Hg^{2+} adsorption efficiency. Experiment conditions: 1.0 mg/L Hg^{2+} solution, 10 min contact time, 500 rpm agitation speed, pH = 6.0, room temperature.

6, t = 10 min) (Fig. 9). It can be observed that the removal efficiency was increased slightly with enhancement of the adsorbent dose from 2–10 μmol. This observation arises from the increasing adsorbent surface area and the availability of Hg^{2+} to adsorption active sites. The adsorption reached a maximum with 10 μmol of adsorbent and the maximum percentage removal was about 88%. Similarly, at a lower concentration of EDT-Fe_3O_4 MNPs (2 μmol), the percentage removal of Hg^{2+} reached 85%. Thus, considering the practical application and cost of the nanoparticles, the concentration of 2 μmol was adopted for the succeeding studies.

3.2.4. Adsorption isotherms

The adsorbent capacity and the driving force of adsorption are essential data for designing an appropriate adsorption treatment process. Thus to obtain basic knowledge of the equilibrium relationship between the solid adsorbent and liquid adsorbate, the most frequently applied adsorption isotherms of Langmuir and Freundlich equations sorption isotherm models are adopted. The Langmuir isotherm [Eq. (2)] assumes monolayer adsorption onto a homogeneous surface with a specific number of equivalent sites, while the Freundlich isotherm [Eq. (3)] is based on the assumption of multilayer adsorption, the equations are expressed as follows [37]:

$$Lanmuir\ modal: \frac{1}{q_e} = \frac{1}{Kq_m} \times \frac{1}{C_e} + \frac{1}{q_m} \quad (2)$$

$$Freundlich\ modal: \ln q_e = \ln K_f + \frac{1}{n} \ln C_e \quad (3)$$

where variable q_e and C_e are the adsorption capacity (mg/g) and metal concentration (mg/L) at equilibrium; q_m is the maximum adsorption capacity (mg/g) and K is the Langmuir adsorption constant (L/ mg), while n and K_f are the Freundlich constants.

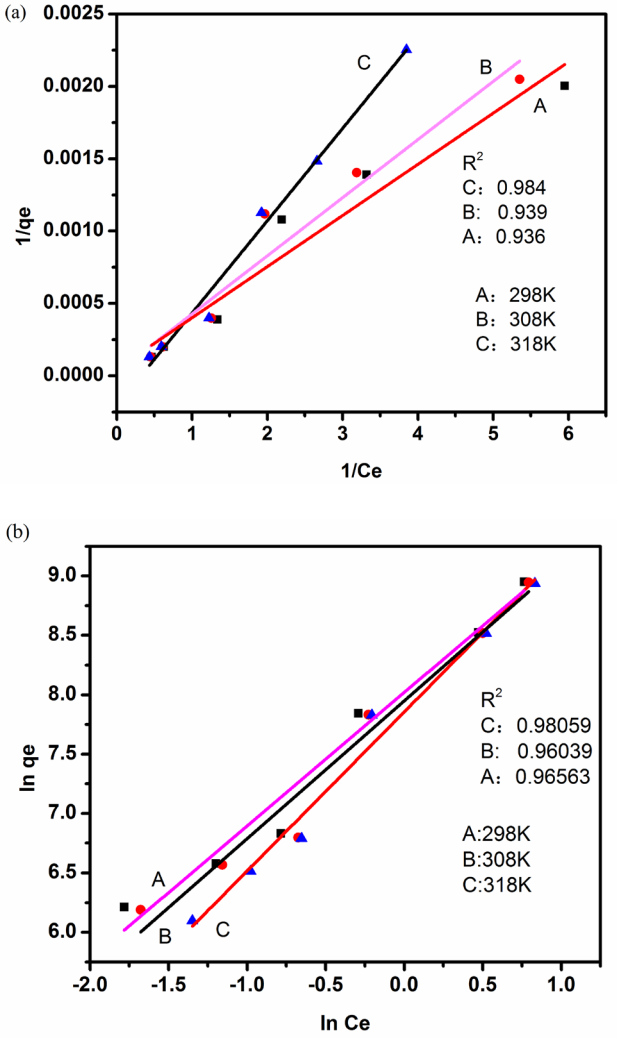

Fig. 10. Langmuir (a) and Freundlich (b) adsorption isotherm fit of Hg^{2+} at 298 K, 308 K and 318 K.

The adsorption isotherm experiments were performed under three different temperatures of 298, 308 and 318 K, the linear fitting curves are displayed in Fig. 10. The regression coefficients (R^2) for the Langmuir model are 0.98, 0.94 and 0.94 at 298 K, 308 K and 318 K, respectively. However, the R^2 values (0.98, 0.96, 0.97) for the Freundlich isotherm at this given temperature are better than Langmuir model. It reveals that Freundlich model is more reliable in describing the adsorption behavior of EDT-Fe_3O_4 MNPs for Hg^{2+} than Langmuir model, which indicates the presence of heterogeneous surface sites in the adsorbent and the multilayer coverage of Hg^{2+} [32].

3.2.5. Adsorption kinetics

The carbon-bonded sulfhydryl (R-SH) group in the EDT molecule creates strong interaction with the mercury ions because of the strong bonding of Hg and S. Therefore, EDT-Fe_3O_4-NMPs can adsorb mercury ions in the aqueous solution. Understanding the kinetics of metal

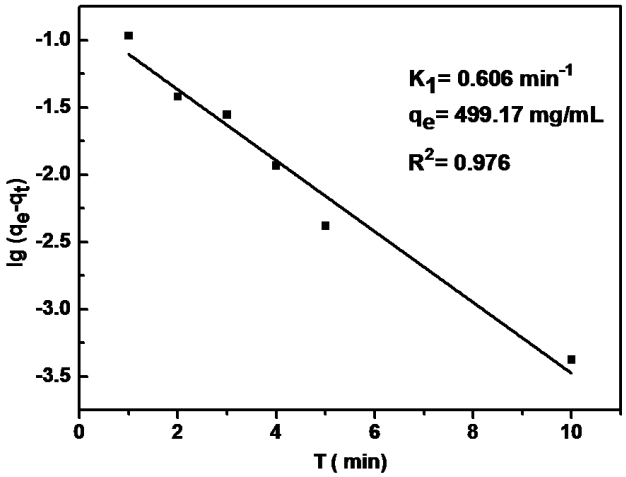

Fig. 11. Pseudo-first-order mode plot for the adsorption of Hg^{2+} onto the EDT-Fe_3O_4 NMPs.

ions removal by EDT-Fe_3O_4 MNPs is of great importance for its practical application. Kinetic models have been developed to investigate the adsorption mechanism and the potential rate-limiting steps, which may include mass transport and chemical reaction processes. The rates at which metal ions move from the solution to the adsorbent surface and accumulate determine the kinetics of adsorption, and hence, the efficiency of the adsorption process [38]. For this purpose, the pseudo-first-order model was used to study the adsorption mechanism of the metal ions on the solid phase. The linear model of the pseudo-first-order model (Eq. 4) is expressed by the following equation [39,40]:

$$\log\left(q_e - q_t\right) = \log q_e - \frac{k_{ad}}{2.303}t \tag{4}$$

where k_{ad} is the pseudo-first-order rate constant (min^{-1}) of adsorption which can be obtained from the straight line plot of log ($q_e - q_t$) versus t, while q_e and q_t are the adsorption capacities of Hg^{2+} (mg/g) at equilibrium and at time t (min), respectively.

The linear plot of the kinetic model for Hg^{2+} is presented in Fig. 11. The pseudo-first order kinetic model fit adsorption data well with $R^2 = 0.976$, indicating that the adsorption of Hg^{2+} onto EDT-Fe_3O_4 NMPs obeys the pseudo-first-order kinetic model for the whole adsorption period. Moreover, adsorption capacity at equilibrium calculated from the pseudo-first order model fitting ($q_{e(cal)}$) was 499.17 mg/mL and k_1 the slope was 0.606 min^{-1}.

3.2.6. Desorption experiment

Desorption of metal ions from adsorbent and regeneration of the adsorbent are a major issue in view of reusability of the adsorbent. For desorption study, the metal ion-loaded EDT-Fe_3O_4 NMPs adsorbent collected with a magnet from the adsorption experiments, and washed with water to remove the unabsorbed metals loosely attached to the vial and adsorbent. Then different concentrations of acetic acid (0.2 M,0.5 M and 1.0 M) as the eluent was added to the separated adsorbent. The final concentration of metal ions in the eluent was determined by spectrophotometer and the final results are shown in Table 1. According to Table 1, it is evident that out of the two eluents, acetic acid had been identified as the best eluent as it had 84% desorption efficiency, whereas ammonia showed a maximum of 11% desorption efficiency. Electrocoagulation [41] and some advanced materials [42] such as graphene oxide functionalized with magnetic nanoparticles [43], multi-walled carbon nanotubes [44] have been reported for removal of mercury in aqueous environments. Compared with these materials, the EDT-Fe_3O_4-NMPs are facile to synthesis and functionalize.

Table 1
Effect of different eluents on desorption recovery (%)

Eluent	Conc. of eluent (M)	Recovery (%)
Ammonia	0.2	2.4
Ammonia	0.5	7.7
Ammonia	1.0	11.3
Acetic acid	0.2	12.7
Acetic acid	0.5	43.1
Acetic acid	1.0	84.8

4. Conclusion

In the present work, a novel kind of surface mercapto modified Fe_3O_4 magnetic nanoparticles (EDT-Fe_3O_4-NMPs) was prepared by a simple co-precipitation method combined with surface modification with EDT agent. The obtained EDT-Fe_3O_4-NMPs are quasi-spherical with an average diameter of about 15 nm and saturation magnetization of 25 emu/g. The Hg^{2+} quickly adsorbed onto EDT-Fe_3O_4-NMPs and adsorption process followed the pseudo-first-order kinetic model. The adsorption process can be better simulated by the Freundlich isotherm to explain the adsorption behavior of Hg^{2+} on EDT-Fe_3O_4-NMPs. In addition, the adsorbent can be separated and recovered by the external magnetic field easily. Its reusability could be achieved by treating the used EDT-Fe_3O_4-NMPs with acetic acid. Although the EDT-Fe_3O_4-NMPs can adsorb the Hg^{2+}, as well known that the -SH also has interactions with Pb^{2+} and Cd^{2+}. The as-prepared material has low selectivity for these three heavy metals. Therefore, the EDT-Fe_3O_4-NMPs would be a potential candidate as a highly efficient and inexpensive adsorbent for Hg^{2+}, Pb^{2+} and Cd^{2+}.

Acknowledgments

This work was supported by the National Natural Science Foundation of China (31501397), the National Key Research and Development Program of China (2016YFD0401204), the Fundamental Research Funds for the Central Universities (JUSRP51714B) and National First-class Discipline Program of Food Science and Technology (JUFSTR20180301, JUFSTR20180303).

References

[1] Y. Liu, M. Chen, H. Yongmei, Study on the adsorption of Cu(II) by EDTA functionalized Fe_3O_4 magnetic nano-particles, Chem. Eng. J., 218 (2013) 46–54.

[2] J. Hou, R. Lu, M. Sun, S.A. Baig, T. Tang, L. Cheng, X. Xu, Effect of heavy metals on the stabilization of mercury(II) by DTCR in desulfurization solutions, J. Hazard. Mater., 217–218 (2012) 224–230.

[3] S. Zhang, Y. Zhang, J. Liu, Q. Xu, H. Xiao, X. Wang, H. Xu, J. Zhou, Thiol modified Fe_3O_4@SiO_2 as a robust, high effective, and recycling magnetic sorbent for mercury removal, Chem. Eng. J., 226 (2013) 30–38.

[4] D.G. Streets, Z. Lu, L. Levin, A.F.H. Schure, E.M. Sunderland, Historical releases of mercury to air, land, and water from coal combustion, Sci. Total. Environ., 615 (2018) 131–140.

[5] Y. Ma, Y. Pang, F. Liu, H. Xu, X. Shen, Microwave-assisted ultrafast synthesis of silver nanoparticles for detection of Hg^{2+}, Spectrochim. Acta. A, 153 (2016) 206–211.

[6] H. Parham, B. Zargar, R. Shiralipour, Fast and efficient removal of mercury from water samples using magnetic iron oxide nanoparticles modified with 2-mercaptobenzothiazole, J. Hazard. Mater., 205–206 (2012) 94–100.

[7] Y. Niu, R. Qu, H. Chen, L. Mu, X. Liu, T. Wang, Y. Zhang, C. Sun, Synthesis of silica gel supported salicylaldehyde modified PAMAM dendrimers for the effective removal of Hg(II) from aqueous solution, J. Hazard. Mater., 278 (2014) 267–278.

[8] J. Sun, Z. Chen, M. Ge, L. Xu, M. Zhai, Selective adsorption of Hg(II) by γ-radiation synthesized silica-graft-vinyl imidazole adsorbent, J. Hazard. Mater., 244–245 (2013) 94–101.

[9] L.R. Varghese, N. Das, Removal of Hg (II) ions from aqueous environment using glutaraldehyde crosslinked nanobiocomposite hydrogel modified by TETA and β-cyclodextrin: Optimization, equilibrium, kinetic and ex situ studies, Ecol. Eng., 85 (2015) 201–211.

[10] D.A. Atwood, M.K. Zaman, Mercury removal from water, Struct. Bond, 120 (2006) 163–182.

[11] S. Carson, Contaminated water: A new solution to mercury removal, FiltrSepar., 44 (2007) 14–15.

[12] J.K. Sikkema, J.E. Alleman, Mercury regulation, fate, transport, transformation, and abatement within cement manufacturing facilities: Review, Sci. Total Environ., 409 (2011) 4167–4178.

[13] J. Gómez-Pastora, E. Bringas, I. Ortiz, Recent progress and future challenges on the use of high performance magnetic nano-adsorbents in environmental applications, Chem. Eng. J., 256 (2014) 187–204.

[14] Z. Tan, L. Sun, J. Xiang, H. Zeng, Z. Liu, S. Hu, J. Qiu, Gas-phase elemental mercury removal by novel carbon-based sorbents, Carbon, 50 (2012) 362–371.

[15] S.I. Lo, P.C. Chen, C.C. Huang, H.T. Chang, Gold Nanoparticle-aluminum oxide adsorbent for efficient removal of mercury species from natural waters, Environ. Sci. Technol., 46 (2012) 2724–2730.

[16] E. Sumesh, M.S. Bootharaju, Anshup, T. Pradeep, A practical silver nanoparticle-based adsorbent for the removal of Hg^{2+} from water, J. Hazard. Mater., 189 (2011) 450–457.

[17] K. Abbas, H. Znad, M.R. Awual, A ligand anchored conjugate adsorbent for effective mercury(II) detection and removal from aqueous media, Chem. Eng. J., 334 (2018) 432–443.

[18] Q.Z. Zhai, Y.Q. Ma, H. Yu, X.H. Liu, SBA-15 for effective removal of mercury(II) from aqueous solution, Asian J. Chem., 23 (2011) 4079–4086.

[19] Y. Zhang, Q. Li, L. Sun, R. Tang, J.P. Zhai, High efficient removal of mercury from aqueous solution by polyaniline/humic acid nanocomposite, J. Hazard. Mater., 175 (2010) 404–409.

[20] G.W. Yang, H.Y. Han, C.Y. Du, Z.H. Luo, Y.J. Wang, Facile synthesis of melamine-based porous polymer networks and their application for removal of aqueous mercury ions, Polymer, 51 (2010) 6193–6202.

[21] N. Dave, M.Y. Chan, P.J. Huang, B.D. Smith, J. Liu, Regenerable DNA-functionalized hydrogels for ultrasensitive, instrument-free mercury(II) detection and removal in water, J. Am. Chem. Soc., 132 (2010) 12668–12673.

[22] N. Siddiqui, J. Don, K. Mondal, A. Mahajan, Development of bamboo-derived sorbents for mercury removal in gas phase, Environ. Technol., 32 (2011) 383–394.

[23] S.A. Ahmed, Alumina physically loaded by thiosemicarbazide for selective preconcentration of mercury(II) ion from natural water samples, J. Hazard. Mater., 156 (2008) 521–529.

[24] D. Pérez-Quintanilla, I. del Hierro, F. Carrillo-Hermosilla, M. Fajardo, I. Sierra, Adsorption of mercury ions by mercapto-functionalized amorphous silica, Anal. Bioanal. Chem., 384 (2006) 827–838.

[25] N. Pourreza, K. Ghanemi, Determination of mercury in water and fish samples by cold vapor atomic absorption spectrometry after solid phase extraction on agar modified with 2-mercaptobenzimidazole, J. Hazard. Mater., 161 (2009) 982–987.

[26] B. Wang, F. Zhang, J. Qiu, X. Zhang, H. Chen, Y. Du, P. Xu, Preparation of Fe_3O_4 superparamagnetic nanocrystals by coprecipitation with ultrasonic enhancement and their characterization, Acta Chim. Sinica, 67 (2009) 1211–1216.

[27] Ministry of Health of the People's Republic of China and Standardization Administration of the People's Republic of China, GB/T 5750.6-2006, Standard Examination Methods for Drinking Water Metal Parameters, 2006.

[28] C.C. Lin, Y.S. Lin, J.M. Ho, Adsorption of Reactive Red 2 from aqueous solutions using Fe_3O_4 nanoparticles prepared by co-precipitation in a rotating packed bed, J. Alloys Comp., 666 (2016) 153–158.

[29] L. Wang, Z. Yang, J. Gao, K. Xu, H. Gu, B. Zhang, X. Zhang, B. Xu, A biocompatible method of decorporation: Bisphosphonate-modified magnetite nanoparticles to remove uranyl ions from blood, J. Am. Chem. Soc., 128 (2006) 13358–13359.

[30] S. Xuan, Y.X.J. Wang, J.C. Yu, C.F. Leung, Tuning the grain size and particle size of superparamagnetic Fe_3O_4 microparticles, Chem. Mater., 21 (2009) 5079–5087.

[31] Y. Zhu, W. Zhao, A.H. Chen, J. Shi, A simple one-pot self-assembly route to nanoporous and monodispersed Fe_3O_4 particles with oriented attachment structure and magnetic property, J. Phys. Chem., 111 (2007) 5281–5285.

[32] G. Jiang, Q. Chang, F. Yang, X. Hu, H. Tang, Sono-assisted preparation of magnetic ferroferric oxide/graphene oxide nanoparticles and application on dye removal, Chinese J. Chem. Eng., 23 (2015) 510–515.

[33] H. Tang, W. Zhou, A. Lu, L. Zhang, Characterization of new sorbent constructed from Fe_3O_4/chitin magnetic beads for the dynamic adsorption of Cd^{2+} ions, J. Mater. Sci., 49 (2014) 123–133.

[34] L.G. Bach, M.R. Islam, J.T. Kim, S. Seo, K.T. Lim, Encapsulation of Fe_3O_4 magnetic nanoparticles with poly(methyl methacrylate) via surface functionalized thiol-lactam initiated radical polymerization, Appl. Surf. Sci., 258 (2012) 2959–2966.

[35] R.M. Patil, P.B. Shete, N.D. Thorat, S.V. Otari, K.C. Barick, A. Prasad, R.S. Ningthoujam, B.M. Tiwale, S.H. Pawar, Non-aqueous to aqueous phase transfer of oleic acid coated iron oxide nanoparticles for hyperthermia application, RSC Adv., 4 (2014) 4515–4522.

[36] H.L. Fan, L. Li, S.F. Zhou, Y.Z. Liu, Continuous preparation of Fe_3O_4 nanoparticles combined with surface modification by L-cysteine and their application in heavy metal adsorption, Ceram. Int., 42 (2016) 4228–4237.

[37] K. Jainae, N. Sukpirom, S. Fuangswasdi, F. Unob, Adsorption of Hg(II) from aqueous solutions by thiol-functionalized polymer-coated magnetic particles, J. Ind. Eng. Chem., 23 (2015) 273–278.

[38] D.H. Reddy, S.M. Lee, Application of magnetic chitosan composites for the removal of toxic metal and dyes from aqueous solutions, Adv. Colloid. Interf. Sci., 201–202 (2013) 68–93.

[39] S.C. Tsai, T.H. Wang, Y.Y. Wei, W.C. Yeh, Y.L. Jan, S.P. Teng, Kinetics of Cs adsorption/desorption on granite by a pseudo first order reaction model, J. Radioanal. Nucl. Ch., 275 (2007) 555–562.

[40] B. Song, P. Xu, G.M. Zeng, J.L. Gong, X.X. Wang, J. Yan, S.F. Wang, P. Zhang, W.C. Cao, S.J. Ye. Modeling the transport of sodium dodecyl benzene sulfonate in riverine sediment in the presence of multi-walled carbon nanotubes, Water Res., 129 (2018) 20–28.
[41] E. Bazrafshan, L. Mohammadi, A. Ansarimoghaddam, A.H. Mahvi, Heavy metals removal from aqueous environments by electrocoagulation process-a systematic review, J. Environ. Health. Sci., 13 (2015) 74–89.
[42] P. Gao, B.B. Gao , J.Q. Gao , K. Zhang, Y.P. Yang, H.W. Chen, Chitosan and its composites for removal of mercury ion from aqueous solution, Prog. Chem., 28 (2016) 1834–1846.
[43] M. Khazaei, S. Nasseri, M.R. Ganjali, M. Khoobi, R. Nabizadeh, A.H. Mahvi, E. Gholibegloo, S. Nazmara, Modeling mercury (II) removal at ultra-low levels from aqueous solution using graphene oxide functionalized with magnetic nanoparticles: optimization, kinetics, and isotherm studies, Desal. Water Treat., 83 (2017) 144–158.
[44] K. Yaghmaeian, R.K. Mashizi, S. Nasseri , A.H. Mahvi, M. Alimohammadi, S. Nazmara. Removal of inorganic mercury from aquatic environments by multi-walled carbon nanotubes, J. Environ. Health Sci., 13 (2015) 55–63.